Chemiluminescence as a diagnostic tool in CO_2 microwave plasma

F. J. J. Peeters[1], H. J. L. Hendrickx[1], A. W. van de Steeg[1], T. W. H. Righart[1], A. J. Wolf[1], G. J. van Rooij[1,2]
W. A. Bongers[1], M. C. M. van de Sanden[1,2]

[1]*Dutch Institute for Fundamental Energy Research, DIFFER, Eindhoven, The Netherlands*
[2]*Department of Applied Physics, Eindhoven University of Technology, Eindhoven, The Netherlands*

Abstract: Vortex-stabilized CO_2 microwave plasma reactors exhibit an expansive afterglow region, contained within a recirculation zone surrounding the plasma. In this work, absolute intensity-calibrated afterglow emission is measured and its composition assigned to two chemiluminescent processes: $O + O \rightarrow O_2 + h\nu$ and $CO + O \rightarrow CO_2 + h\nu$. Using spectral models of both components, the species composition of the afterglow can be established.

Keywords: CO_2 plasma, afterglow, emission spectroscopy

1. Introduction

Microwave plasmas offer promising efficiency and scalability for the conversion of CO_2 to CO in industrial systems for the production of solar fuels [1].

The configuration of the CO_2 microwave plasma reactor is shown in **Fig. 1** and consists of a quartz tube with a tangential injection nozzle on one end, with pumping occurring on the other end. The quartz tube passes through a WR-340 waveguide, where 2.45 GHz microwave radiation is used to sustain the plasma. Typical operating conditions are pressures of 50 – 500 mbar, absorbed microwave powers of 400 – 1400 W and CO_2 flow rates of 4 – 24 standard liters per minute.

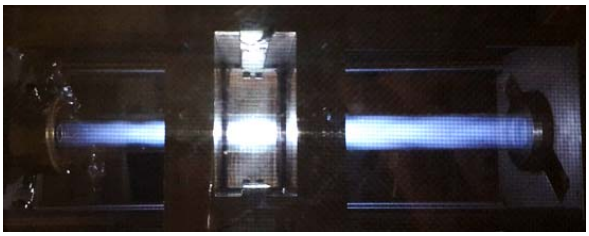

Fig. 1 Photograph of the vortex-stabilized microwave plasma. Tangential injection of CO_2 occurs on the left-hand-side, plasma is visible within the waveguide at the center, while pumping occurs on the right-hand-side. Afterglow emission is visible throughout the reactor tube.

The tangential injection of CO_2 produces a cold, outer vortex near the tube wall, with streamlines spiraling downwards towards the pumped end of the tube. Within the center of the tube, a secondary, recirculating vortex is formed which has no streamlines connecting directly to the exhaust. This approach is made necessary by the high gas temperatures produced by the plasma, which are typically in the range of 3500 – 6000 K [2].

While this configuration allows for stable, high-power-density plasma (up to 1 GW/m^3), with energy efficiency of CO production up to 45% and conversion yields of 15% of CO_2 input flow [1], it is difficult to assess the rate-limiting steps for CO production. The plasma itself is sufficiently hot to ensure full dissociation of CO_2 into CO and O, but the eventual yield of CO from the reactor is dependent on its trajectory within the inner recirculating vortex, the mixing of species between inner and outer vortex, as well as the gas temperature gradients encountered along the way.

To improve our understanding of the overall CO production process, a diagnostic which allows for mapping the composition and gas temperatures in the regions surrounding the plasma is proposed: absolute broadband emission spectroscopy of the afterglow.

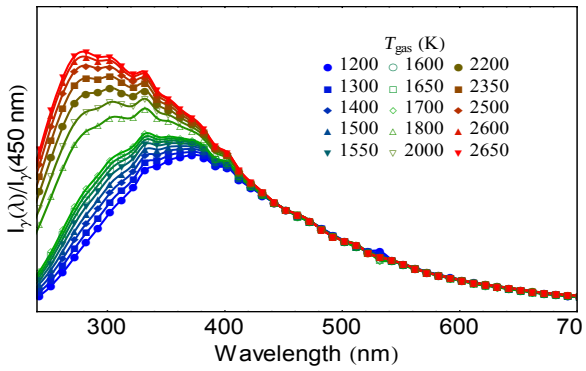

Fig. 2 Typical afterglow emission spectra normalized at λ = 450 nm, obtained at various gas temperatures within the afterglows of 200 and 250 mbar plasmas. Gas temperatures are measured independently using rotational Raman scattering on CO_2.

2. Afterglow emission in CO_2 microwave plasma

Typical absolute intensity-calibrated afterglow emission spectra are depicted in **Fig. 2**. By simultaneously measuring local gas temperatures using rotational Raman scattering, the dependence of this emission on temperature can be studied. The afterglow emission is composed of roughly equal contributions from two chemiluminescent processes: recombination of atomic oxygen with (i) another oxygen atom, or (ii) with carbon monoxide. Process (i) is a 2-particle *inverse pre-dissociation* reaction, whereby oxygen atoms combine along a repulsive potential energy surface with a transition to the B $^3\sum_u^-$ state [3]:

$$O + O \rightarrow O_2(1\ ^3\prod_u) \rightarrow O_2(B\ ^3\sum_u^-) \rightarrow O_2 + h\nu, \qquad (1)$$

which produces radiation between 160 – 490 nm.

Process (ii) involves 3-particle recombination of an oxygen atom, carbon monoxide and a third particle M,

followed by transition to a radiative state and quenching on another third particle:

$$CO + O + M \leftrightarrow CO_2(1\,^3A'\textstyle\sum_u^+) + M, \quad (2a)$$

$$CO_2(1\,^3A'\textstyle\sum_u^+) \leftrightarrow CO_2(1\,^1A''\textstyle\prod_g), \quad (2b)$$

$$CO_2(1\,^1A''\textstyle\prod_g) + M \rightarrow CO_2 + M \text{ and} \quad (2c)$$

$$CO_2(1\,^1A''\textstyle\prod_g) \rightarrow CO_2 + h\nu. \quad (2d)$$

Overall, reactions (2a-d) result in an effective 2-particle process for the photon emission rate, with emission between 250 – 800 nm [4]. Reactions (2a-d) lead to spectral distributions for $CO + O \rightarrow CO_2 + h\nu$ which are, to a good approximation, independent of pressure or temperature [4]. Example spectral fits of measured data are depicted in **Fig. 3**, with the CO + O component depicted as green lines. The area under these curves, i.e. the total emission intensity, is proportional to the CO and O densities, with an activation barrier for emission of about 2000 K.

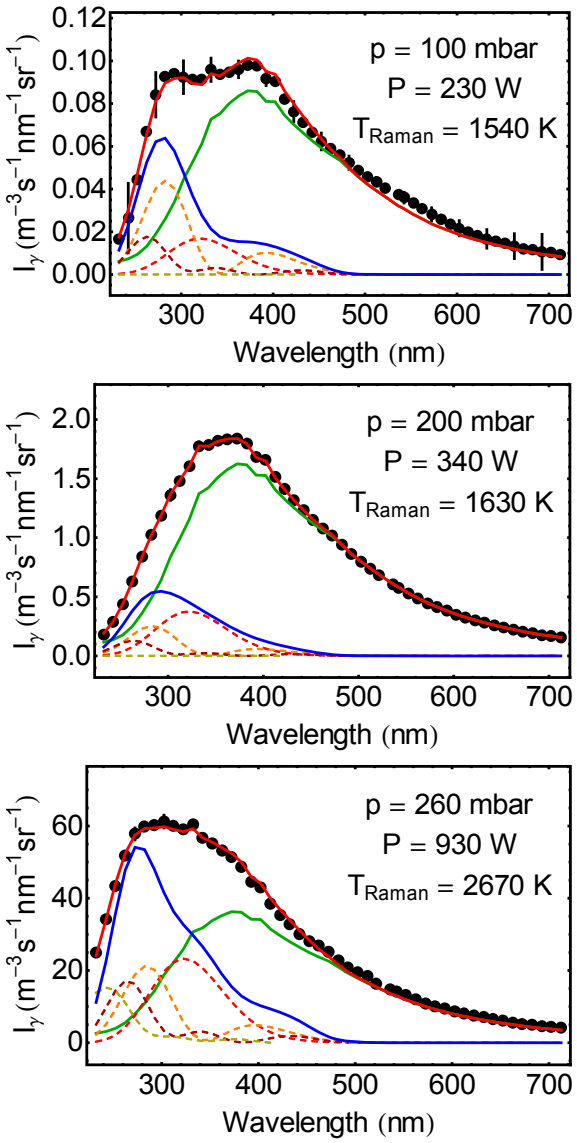

Fig.3 Preliminary fits of afterglow emission at 100, 200 and 260 mbar, with $CO + O \rightarrow CO_2 + h\nu$ (green line), $O + O \rightarrow O_2 + h\nu$ (blue line) and total emission (red line). The dashed lines indicate separate contributions to the O + O emission from $O_2(B)$ in $\nu = 0, 1, 2$ and 3 vibrational states.

The fitted spectral distributions resulting from reaction (1) are indicated by blue lines in **Fig. 3**. The $O_2(B\,^3\textstyle\sum_u^-)$ states formed in reaction (1) have an approximate radiative lifetime of 0.3 – 1.0 µs, which is about 2 orders of magnitude longer than the collision time between O_2 and other gas particles in the afterglow. This implies significant changes can take place in the vibrational distribution of $O_2(B\,^3\textstyle\sum_u^-)$ via quenching processes occurring between formation of the excited state and emission of a photon. With the initial vibrational distribution of $O_2(B\,^3\textstyle\sum_u^-)$ already being dependent on the kinetic energy of the recombining atomic oxygen, this leads to significant variation in the observed $O + O \rightarrow O_2 + h\nu$ emission with pressure and gas temperature.

In the present work, a predictive model is developed for the emission from reaction (1) using only temperature and pressure as input, with an additional effort to link the total photon emission rate from this reaction to the concentration of atomic oxygen in the afterglow. Combined with the much simpler model for emission from reactions (2a-d), the concentration of carbon monoxide can be similarly obtained.

3. Conclusions and outlook

By measuring absolute photon emission in the afterglow of a CO_2 microwave plasma, and fitting the resulting spectra to (temperature-dependent) models for chemiluminescence, both local CO and O densities within the afterglow can be determined. This can provide insight into the distribution of back-reactions to CO_2 and O_2 within the inner recirculating vortex. The method can be expanded to 2D imaging of the afterglow at various wavelengths, allowing for a relatively fast mapping of afterglow composition over a wide range of operating conditions.

4. References

[1] W. A. Bongers et al, Plasma-driven dissociation of CO2 for fuel synthesis Plasma Process. Polym. 1–8, 2016

[2] N. den Harder, Homogeneous CO2 conversion by microwave plasma: Wave propagation and diagnostics Plasma Process. Polym. 1–24, 2016

[3] J. F. Babb and A. Dalgarno, Radiative association and inverse predissociation of oxygen atoms Phys. Rev. A 51 3021–6, 1995

[4] A. M. Pravilov and L. G. Smirnova, Temperature dependence of the spectral distribution of the rate constant of chemiluminescence in the reaction O(3P) + CO → CO2 + hν Kinet. Catal. 22 641–6, 1981